

Single Pass Stripline Beam Position Monitor Design, Fabrication and Commissioning

Y.-R. E. Tan, D. Wang, E. Van Garderen and J. McKinlay

Australian Synchrotron, 800 Blackburn Road, Clayton 3168, Victoria, Australia

Abstract. To monitor the position of the electron beam during transport from the Booster Synchrotron to the Storage Ring at the Australian Synchrotron, a stripline Beam Position Monitor (BPM) has been designed, fabricated and installed in-house. The design was based on an existing stripline in the Booster and modified for the transfer line with a particular emphasis on ensuring the line impedance is properly matched to the detector system. The initial bench tests of a prototype stripline showed that the fabrication of the four individual striplines in the BPM was made precisely, each with a measured standing wave ratio (SWR) of 1.8 at 500 MHz. Further optimization for impedance matching will be done for new stripline BPMs. The linearity and gain factor was measured with the detector system. The detector system that digitizes the signals is an Instrumentation Technologies Brilliance Single Pass [1]. The results show an error of 1 mm at an offset (from the electrical centre) of 10 mm when a linear gain factor is assumed and an RMS noise of ~150 um that decreases to < 10 um with increasing signal intensity. The results were under our requirements for the transport line. The commissioning results of the stripline will also be presented showing a strong signal for an electron beam with an estimated integrated charge of ~50 nC with a position stability of 28 um (horizontal) and 75 um (vertical).

1 Introduction

To monitor the position of the electron beam during transport from the Booster Synchrotron to the Storage Ring (BTS) at the Australian Synchrotron, a stripline Beam Position Monitor (BPM) has been designed, fabricated and installed in-house. The BPM uses four capacitive pick-ups that generate a voltage signal when an electron beam travels past. These pick-ups consist of four striplines arranged in a “square” configuration to calculate the transverse location of the passage of the electron beam relative to the striplines.

2 Design And Fabrication

An existing design for a quarter-wave ($\lambda/4$) stripline was modified to accommodate new constraints in the BTS. The length of the stripline was chosen to optimise the signal received by the BPM electronics at 500 MHz. The mechanical design is shown in Figure 1 with the arrangement of the four pick-ups. The calculation of the transverse position is given by

$$X = k_x \frac{(A + D) - (B + C)}{A + B + C + D} \quad Y = k_y \frac{(A + B) - (C + D)}{A + B + C + D} \quad (1)$$

where k_x and k_y are gain/conversion factors that give X and Y in meters and A, B, C and D are the peak voltages generated by the electron beam as it travels past the stripline.

In addition to designing the appropriate length of the stripline pickup, the characteristic impedance of the striplines must also be designed to match the electronics (50Ω) to minimise signal loss and distortions. The equation used to model the impedance is [2],

$$Z_0 \Big|_{f=0} = \frac{119.9 \pi}{2 \sqrt{\epsilon_r}} \left[\frac{w}{2h} + \frac{\ln(4)}{\pi} + \frac{\ln(e \pi^2 / 16)}{2\pi} \left(\frac{\epsilon_r - 1}{\epsilon_r^2} \right) \right. \\ \left. + \frac{\epsilon_r + 1}{2\pi \epsilon_r} \left(\ln \left(\frac{\pi e}{2} \right) - \ln \left(\frac{w}{2h} + 0.94 \right) \right) \right]^{-1} \quad (2)$$

where h is the height of the strip from the ground plane (chamber wall), w the width of the strip, ϵ_r is the dielectric constant (in this case of air), Z_0 the characteristic impedance at $f = 0$ Hz and e is the Euler’s constant. In this particular design $w = 15.7$ mm and $h = 3.0$ mm giving $Z_0 = 48 \Omega$. This was an error in the initial design, the ideal would have been letting $h = 3.17$ mm which gives $Z_0 = 50 \Omega$. The assumption used for the modeling of the impedance is that ϵ_r and Z_0 are frequency independent. Frequency dependent equations were used

however the change at 500 MHz did not make a significant difference.

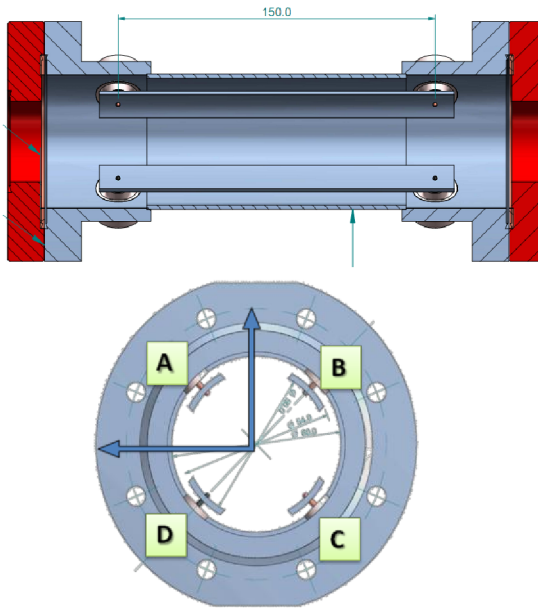


Fig. 1. Design of the BPM with the four striplines, labelled, A, B, C and D. These striplines are connected to SMA UHV feed-through connectors from Kyocera. The full length of the stripline is 168 mm.

2.1 Materials and Fabrication

The main body of the vacuum chamber and the strips were purchased as individual pieces of tubing and UHV flanges made from stainless steel (SS304). The UHV feed-through coaxial connections that connect the strips to female SMA ports are Kyocera SMA-R units with a cut-off frequency at 6.5 GHz. All parts were precision machined to tolerances of 50 μm or better with surface finishes of 1.6 μm Ra or better. Custom position jigs were constructed to hold the coaxial connector as well as the strips in position with a tolerance of less than 100 μm . In the final position the pieces were TIG welded, taking care around the coaxial connectors as extreme heat can damage the ceramic seal in the connectors. Upon completion the unit's inner surface was electrochemically polished to remove any residuals and oxides. Only then was the unit ready for the test-bench.

3 Test-Bench Measurements

To determine the frequency response of the striplines, one approach is to send a short pulse (≤ 100 ps) along a wire to mimic an electron bunch and measure the response to the pseudo impulse on a spectrum analyser. The equipment to generate such pulses were not available, so an Agilent E5052a network analyser was used to measure the transmission efficiency by connecting port 1 to one end of a stripline with the other end terminated with a 50 Ω load. Port 2 was connected to a second stripline in a similar fashion. The transmission measurement (S12) gives a measure of the frequency

response of the stripline by using one to simulate the electron beam and the other as a monitor.

The results of the measurements in Figure 2 showed nodes that was expected at 1 GHz and its harmonics. The node was measured at 947 MHz ($\lambda/4 = 158$ mm) and is likely a consequence of edge protruding past the connection point increasing the total effective length and shifting the node. This is not a significant issue as the peak transfer at 500 MHz would not change by much with a node shifted to exactly 1 GHz. The observed increase in the transfer efficiency above 2.66 GHz only for symmetrical combinations of striplines is due to the excitation of the lowest transverse electric mode (TE11) for the central circular chamber with an internal diameter of 60 mm. The TE11 mode has electric fields that are in the transverse direction (eg. Vertical or horizontal fields) and are not radially symmetric, therefore the TE11 mode can only be excited by two opposing striplines (e.g. A-C or B-D) and not by striplines positioned adjacent to each other (e.g. A-B or B-C). The frequency of the lowest TE11 mode is calculated using,

$$f_{TE11} = 1.841 \frac{c}{\pi d} \quad (3)$$

where c is the speed of light and d the diameter of the circular chamber.

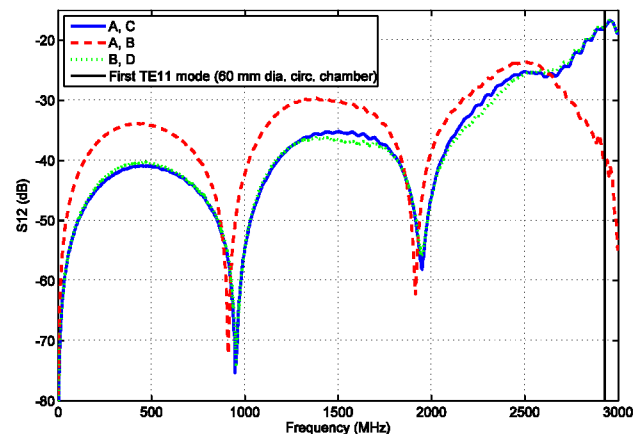


Fig. 2. BPM frequency response from S12 measurements with different combinations of striplines. Symmetrical combinations show a marked increase above 2.66 GHz while asymmetrical combinations do not exhibit this behaviour. The lowest frequency TE11 mode (2.9 GHz) for 60 mm diameter circular chamber is shown.

In the same setup, reflection measurements (S11) were made and plotted in a Smith Chart in Figure 3. The measurement show the stripline is purely resistive at 430 MHz with a real impedance of 31 Ω . At 500 MHz the real impedance is 28 Ω with a small inductive component. This is quite far from the expected impedance of 48 Ω and is likely in part due to the changing internal geometry at the connection between the central pipe and the flanges on either side.

The impedance mismatch to a 50 Ω terminated detector results in a Standing Wave Ratio (SWR) of 1.8 at 500 MHz, meaning about 10% of the power at 500 MHz will be reflected internally. This will cause

unwanted reflections in the system and distort the original signal.

The RF measurements show clearly that there are improvements to be made. The deviations from the expected values are unexplained and simulations of the as-built system are underway to find ways of optimising the system.

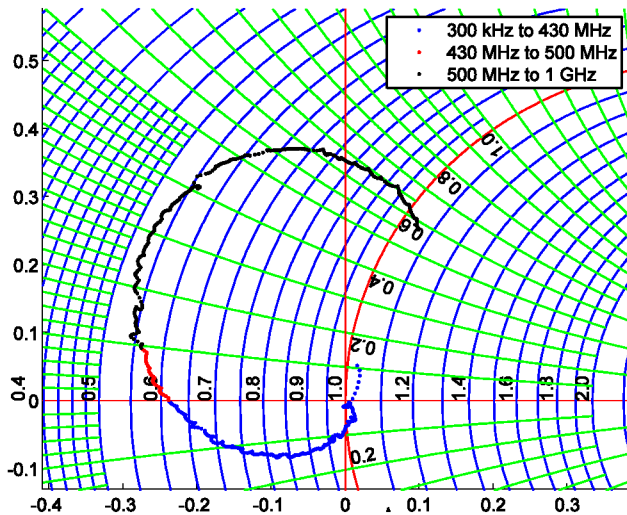


Fig. 3. S11 measurement plotted at a Smith Chart. The strip is purely resistive at 430 MHz (31 Ω) rather than at 500 MHz (28 Ω + small inductance).

3.1 Stretched Wire Measurements

The gain factors in Equation 1 are measured for the BPM using a wire connected to a signal generator to simulate the passage of multiple electron bunches. It is interesting to note the profile of pulse in Fig 4 measured from the stripline showing a coupling factor of ~1% and as expected from the poor matching impedance some ringing.

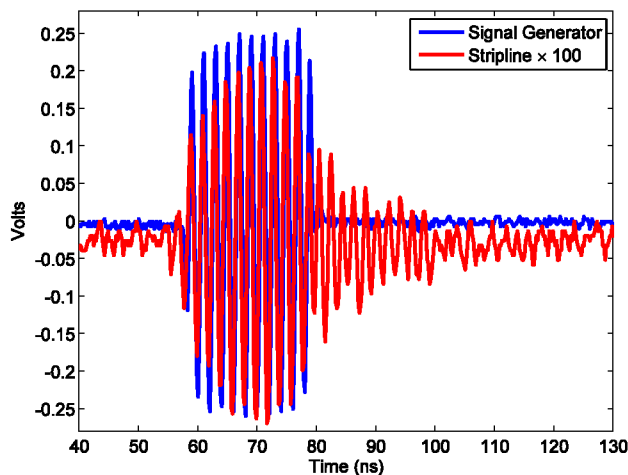


Fig. 4. Gated 500 MHz signal (20 ns pulse) generated by an arbitrary waveform generator and the corresponding signal on a stripline pick-up (scaled by a factor 100).

The final setup is shown in Figure 5 with a Libera Brilliance Single Pass (Libera) [1] used to digitize the signal and calculate X and Y positions. The stretched wire is moved and its position is recorded by two linear probes

with a resolution of 20 μm. The correlation between the measured wire position and the position calculated by Libera is shown in Fig 6. The results show the expected constant gradient such that $\Delta X_{libera}/\Delta X_{real} \approx 2.16$ at $Y=0$ and $\Delta Y_{libera}/\Delta Y_{real} \approx 2.15$ at $X=0$.

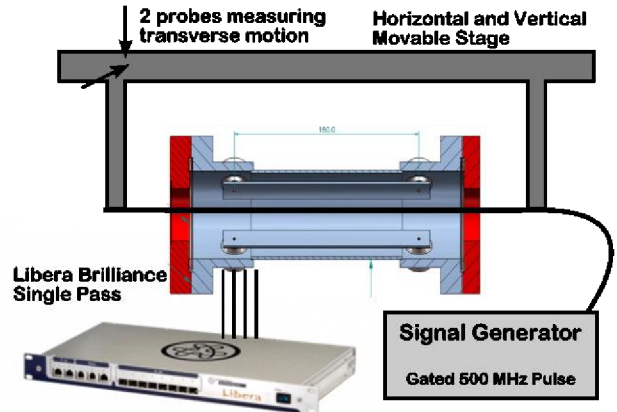


Fig. 5. Stretched wire setup with a signal generator generating a 500 MHz sine wave lasting for 20 ns to simulate the passage of multiple electron bunches. The BPM is connected to a Libera Brilliance Single Pass that digitizes the signal and calculates the X and Y position of the wire. As the stretched wire is translated using the movable stage the positions from the Libera are recorded as a function of the movement of the wire measured by the two linear probes ($\pm 20 \mu\text{m}$).

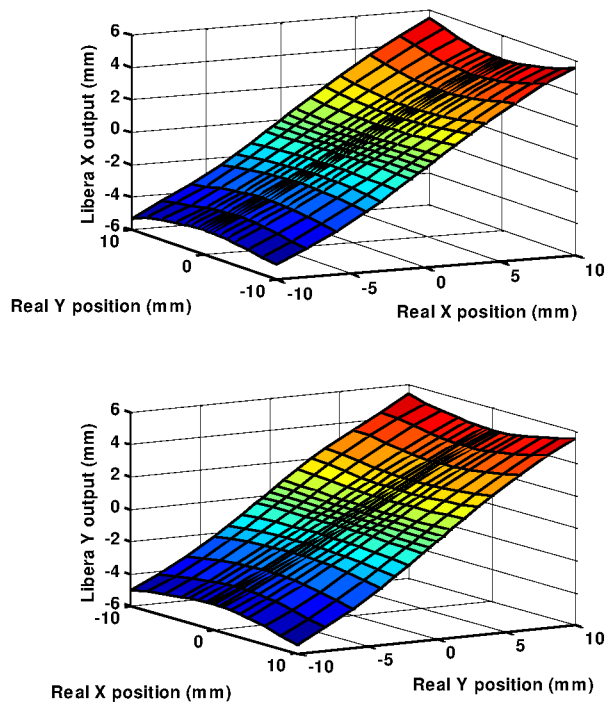


Fig. 6. Libera calculated positions plotted against the measured motion of the wire. There is a fairly linear gradient between X_{libera} and X_{real} around $Y=0$. Nonlinearities begin to increase the further off Y -axis the beam travels. The converse is true for the Y position measurements.

The calibrated gain factors are calculated by multiplying the gain set for the measurement, $k_x = k_y = 10,000,000$

nm, by the average of the measured gradients (2.155). This gives $k_x = k_y = 21,550,000$ nm. Assuming this constant gain, the data in Fig 6 indicate that at beam offsets of 10 mm in either plane the expected position error is ~ 1 mm. If necessary this data can be used in a look up table to linearise the measured Libera positions.

Another important factor is the noise floor of the system. At the lowest signal intensity that can be detected by the Libera the RMS noise on the position was measured to be $150 \mu\text{m}$ (gain setting of -53 and maximum ADC count of 1600 out of 32k). In the middle of the range the RMS noise was $< 10 \mu\text{m}$ (gain setting of -20 and maximum ADC count of 15,500). The BPM was installed and commissioned with the Libera unit and the measured calibration factors.

4 Initial Commissioning Results

The stripline BPM was installed in the BTS and tested with a 150 ns bunch train. The raw ADC data shown in Figure 7 shows the bunch train of 150 ns (20 samples) followed by ~ 240 ns of ringing (30 samples). Finally a second pulse is also observed at an offset of 960 ns (120 samples). If the second pulse is a reflection of the original signal, the time of 960 ns (cable specification of 3.97 ns/m) corresponds to the signal travelling a total of 240 meters. The cable laid between the Libera and BPM is too short for the pulse to be internal reflections. The delay is also too long for the pulse to be a second train of electron bunches. The duration the extraction kicker is “on” at the start of the BTS defines the time window for the electrons to enter the BTS. The width of the kicker is only 200 ns wide so it cannot be a second train of electrons. Fortunately the secondary pulse can be excluded from the calculations so in the meantime it is not of concern.

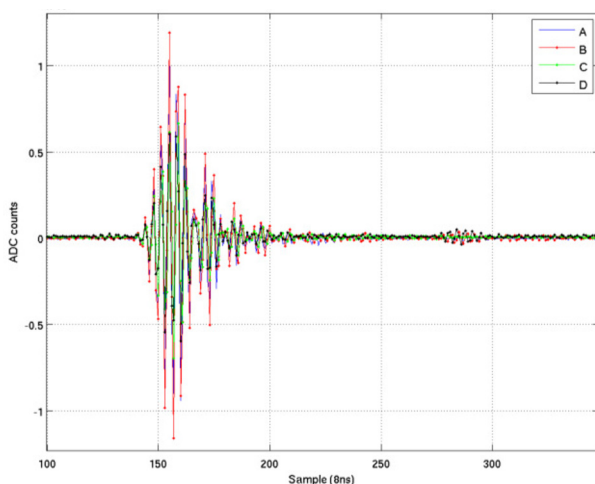


Fig. 7. Raw ADC counts from the Libera for the four pick-ups showing ringing after the bunch passes and a secondary pulse 960 ns after the first pulse passes.

The measured beam stability during one operation period was shown to be $< 70 \mu\text{m}$ where the estimated integrated charge of the electron beam was ~ 50 nC. With a strong signal the expected resolution of the electronics is $< 15 \mu\text{m}$. This meets the present requirement for beam

stability in the BTS. The results here match the results at other light sources [3]. Based on these measurements it is expected that the electronics will be sensitive enough to measure the beam position for charges as low as 0.5 nC with a resolution of at least $150 \mu\text{m}$. The BPM will be used to monitor drifts in the beam position to ensure maximum transfer efficiencies are maintained.

5 Discussion and Future Direction

The results from the RF measurements were not satisfactory with measured impedances well short of the required 50Ω . Simulations will be needed to find the optimal configuration to have a matching 50Ω system [4] as well as improvements in the measurement technique to identify and characterise the impedances [5].

This BPM is the first of three that will be made and installed in the transfer lines at the Australian Synchrotron. The knowledge and experience will be used to improve the current design and eventually work towards designing resonant striplines [6] that can reach single bunch resolution of the order $10 \mu\text{m}$ for charges as low as 10 pC.

Acknowledgements

Thanks to Robert Rostan who did a fantastic job on machining and welding the stripline BPM.

References

1. A. Kosicek, M. Znidarcic, S. Bassanese, *PAC Proceedings*, p 3579 (2009).
2. R. K. Hoffmann, *Handbook of Microwave Integrated Circuits*, (1987).
3. A. Stella, et al., *DIPAC Proceedings*, p 306 (2009).
4. C. Deibele, S. Kurennoy, *PAC Proceedings*, p 2607 (2005).
5. M. Dehler, *DIPAC Proceedings*, p 286 (2005)
6. A. Citterio, et al. *DIPAC Proceedings*, p 71 (2009).